The response of steroid estrogens bioavailability to various sorption mechanisms by soil organic matter extracted with sequential alkaline-extraction method from an agriculture soil

Xiaoming Song[a], Zhipeng Zhang[b,*], Yujuan Wen[a], Wei Zhang[c], Yi Xie[d], Nan Cao[b], Dong Sun[b], Yuesuo Yang[a,e]

[a]*Key Laboratory of Regional Environment and Eco-restoration, Ministry of Education, Shenyang University, Shenyang 110044, China*

[b]*Chengdu Center of Hydrogeology and Engineering Geology, Sichuan Bureau of Geology & Mineral Resources, Chengdu 610081,China*

[c]*College of Engineering, Swansea University, Bay Campus, Swansea SA1 8EN, UK*

[d]*Liaoning Provincial Ecology & Environment Monitoring Center, Shenyang 110161, China*

[e]*College of New Energy and Environment, Jilin University, Changchun 130012, China*

**Correspondence: zzpwss123@126.com; Tel.: +86-431-88502850 (Y.Y.)*

ABSTRACT: The long-term groundwater contamination risks posed by steroidal estrogens (SEs) in animal-manured agricultural soils are closely associated with the soil organic matter (SOM) content and composition. In this study, the bioavailability of estrone (E1) and 17β-estradiol (17β-E2) under different sorption mechanism in humic acids (HA1 and HA2) and humin (HM) extracted with sequential alkaline-extraction technique (SAET) were examined. These SOMs extracted by SAET showed various properties and sorption characteristics for SEs. The alkyl carbon and condensed SOM increased during SAET, but aromatic carbon decreased and the same trend for polarity. Quick sorption was the major SEs sorption mechanism on HA1 and HA2, which contributed more than 69%; whilst slow sorption rate was about 50% in soil and HM. The logK_{oc} values were proportional to the TOC of SOM according to Freundlich fitting, and the sorption capacity of sorbent for E1 and 17β-E2 was related to the logK_{ow} values, indicating that the main mechanism controlling the SEs sorption was hydrophobic interaction. The larger micropore volume of HM and soil was more conducive to the micropore filling of SEs. Meanwhile, the specific sorption of SEs on condensed domain of SOM was the main reason for the strong desorption hysteresis and slow sorption in HM and soil. The SEs degradation rate was positively correlated with the contribution rate of quick adsorption and negatively correlated with the contribution rate of slow adsorption, indicating that the bioavailability of SEs sorbed by hydrophobic interaction was higher than that of micropore filling or specific sorption, which was also the reason for the low bioavailability of SEs in HM and soil. This work confirms the regulation of on-site SOM compositions and their properties on SEs sorption and bioavailability. Characterization of these details is crucial for the improved prediction of long-term risks to groundwater.

Keywords: Steroid Estrogens, Sorption, Bioavailability, Soil Organic Matter, Risk

1. Introduction

Steroidal estrogens (SEs) such as E1 (estrone) and 17β-E2 (estradiol) are commonly found in agricultural soils and groundwater after fertilization with livestock and poultry manure (Gall et al., 2015; Fang et al., 2016; Zhao et al., 2019). Their high bioactivity may cause endocrine disruption effects on the agroecological system, even following exposure to low SEs concentrations (Adeel et al., 2017; Zhao et al., 2019; Wei et al., 2020). Although gains have been made through organic green agriculture in reducing chemical fertilizer application risks, these can be offset by greater environmental risks from SEs posed by increased manure application. As a result of the incomplete sorption and biodegradation in the vadose zone (Song et al., 2018; Zhao et al., 2019), underlying groundwater resources are at risk of SEs contamination through leaching from soils (Citulski et al., 2010; Yang et al., 2021). Improved understanding of sorption and bioavailability controls on the accumulation and decline of legacy SEs sources in agricultural soils and their regulation of groundwater risks is crucial.

The sorption mechanism of SEs in soil is complex due to the heterogeneity of soil components. Especially the origin, type, and the distribution and structure of the functional groups of soil organic matter (SOM), including humic acid (HA) and humin (HM), play a central role in the sorption of SEs, which have a significant impact on the bioavailability of SEs (Sangster et al; 2015; Alizadeh et al., 2018; Yu et al., 2020; Sun et al., 2010). A few studies have confirmed that SEs sorption affinity has a positive correlation with SOM content and the octanol-water partition coefficient (K_{ow}) of SEs, supporting the dominance of hydrophobic interaction mechanisms (Karnjanapiboonwong et al., 2010; Mashtare et al., 2011). However, further sorption mechanisms must exist because of the presence of polar functional groups both in SEs and humic substances (Sun et al., 2012; Gall et al., 2016). For instance, the dominant role of aromatic carbon versus aliphatic carbon in SOM controlling the sorption of SEs remains unresolved (Sun et al., 2008; Jiang et al., 2017). The sorption of SEs may be significantly influenced by their polar hydroxyl function on the benzene ring of SEs molecules or their π-π binding (Takigami et al., 2011; Bedard et al., 2014; Zhang et al.,

2018; Zhao et al., 2020). The feature of SEs sorption on HA or HM is often nonlinear, which is attributed for the specific polar interaction (H-bonding) or pore-filling (Lima et al., 2012; Zhang et al., 2017). Soil minerals and its heterogeneity also affect sorption (Tong et al., 2019; Xu et al., 2020). The sorption capacity of SEs on iron oxides and clay minerals is governed by the content of their ion-exchange materials (Thanhmingliana et al., 2016; Shi et al., 2017), whereas the sorption on montmorillonites displayed interlayer spacing decrease, thereby supporting incorporation of SEs into the clay interlayer space and producing slow sorption (Sun et al., 2017). Therefore, further investigation of the sorption behavior of SEs in a real agricultural soil (in preference to artificial, commercial products) is needed to evaluate SEs bioavailability and transport in the agricultural system. To our knowledge, related research remains surprisingly limited.

The bioavailability of SEs in agricultural soil that are closely related to biodegradation is another important factor affecting their environmental risk because of their nonpersistent properties (Stumpe et al., 2010; Zheng et al., 2012). The bioavailability of contaminants refers to the accessibility of microorganisms or extracellular enzymes in soil and groundwater, which is controlled by the concentration of directly available contaminants and the rate of conversion from potentially available contaminants (Wang et al., 2021). As a result of the heterogeneity of soil components and the complexity of the hydrophobic organic contaminant (HOCs) sorption mechanism on SOM, there may be considerable differences in related bioavailability, which leads to the different opportunities for the utilization of sorbed and free HOCs by microorganisms (Zhang et al., 2018; Gámiz et al., 2018). It is generally believed that only free SEs can be effectively degraded by soil microorganisms, while sorbed SEs need to be desorbed from the solid phase before utilization (Fan et al., 2007). In particular, soil with high SOM content may reduce the bioavailability and biodegradation rates due to irreversible sorption (Lee et al., 2011). However, Combalbert et al. (2010) suggested that soils with different sorption capacities have little influence on the biodegradation of SEs, and the sorbed SEs could be freely desorbed to the liquid phase and degraded. In addition, the degree of isolation of HOCs

increases significantly with the time spent in contact with the soil, a process known as aging, which may increase desorption resistance and reduce the bioavailability of HOCs (Xu et al., 2018). The response of SEs bioavailability to sorption mechanism and to sorption aging with different SOM remains unclear, and is thus the key scientific problem to be solved in the current study.

Thus, we hypothesized that the differences in composition and structure of SOM fractions can result in different controls on the SEs sorption, thereby different bioavailability of sorbed SEs. The main objectives of the present research were to (1) investigate controls on the sorption and desorption of E1 and 17β-E2 in a real agricultural soil and in its component SOM fractions, (2) characterize the conformation and functional groups of SOMs to gain insights into the mechanism of nonlinear and slow sorption of SEs, and (3) explore the effect of sorption behavior on SEs bioavailability in soil and clarify the possible mechanisms related to differences in SOM properties and aging processes. The findings of this work could provide theoretical support for guiding the sustainable development of agriculture and controlling the risk of SEs contamination of groundwater from agricultural sources.

2. Materials and methods

2.1. SEs solutions, agricultural soil, and soil bacterial suspension

The selected sorbates, E1 and 17β-E2, are commonly detected in farmyard manure and agricultural soil (Adeel et al., 2017), and their physicochemical properties are listed in Table S1. E1 (≥99.5%) and 17β-E2 (≥98.4%) were purchased from Sigma-Aldrich (USA). The stock solutions of individual SEs were prepared by dissolving each compound in methanol at a concentration of 1000 mg/L before being stored at −20 °C prior to use.

An agricultural silt loam (9.71% clay, 51.91% silt, and 38.38% sand) was collected from a rural farm in Shenyang, Northeastern China, where maize, vegetables, and fruits are predominantly grown. In our previous investigation (Song et al., 2018), the total concentrations of both SEs in the farm soil were 39.3–112.7 ng/g, compared with

manure at 85.6–357.3 ng/g. For this study, the soil samples without SEs used for SAET of SOM and batch experiments were collected from 0–10 cm soil depth around the edges of the farm where manure had not been applied; however, the soil microbial suspension was prepared using the SEs-containing soil for bioavailability experiment. The fresh soil was air-dried, passed through a 2-mm sieve, and stored at 4 °C before the sorption and bioavailability experiments. The soil samples were treated by sterilization and non-sterilization. For the sterile treatment, soils were autoclaved at 120 °C for 30 min three successive times.

The soil microbial suspension was prepared as follows: 10.0 g non-sterile soil and 20 mL sterile water were mixed well in a 200 mL amber reagent bottle and sealed, followed by incubating at 30 °C in the dark for 3 days. After 80 mL of sterile water was added, the slurry was stirred at 30 °C, 180 rpm for 1 h. Finally, the slurry was centrifuged at 1000 rpm for 10 min to collect the supernatant as a soil microbial suspension.

2.2. Sequential alkaline-extraction technique (SAET)

The SAET method, a modification of the standard method of the International Humic Substances Society, was conducted for the isolation of HA and HM fractions from the agricultural soil (Swift et al., 1996); in brief, (1) soil equilibration was set to pH 1–2 and adjusted with 0.1 M HCl to a ratio of 10 mL liquid to 1 g dry sample, then the suspension was shaken for 1 h at 70 °C; (2) residue was separated by centrifugation and neutralized to pH 7 under a N_2 atmosphere; (3) the alkaline suspension was shaken at 70 °C for 24 h and each supernatant was collected by centrifugation. The above steps were repeated until the supernatant became light yellow or colorless, allowing the HM to be obtained as a precipitate. The supernatant was acidified with 6 M HCl to pH 1–1.5 and left to stand for 12 h, followed by centrifugation to separate the HA (precipitate). The HA was suspended in 0.1 M HCl/0.3 M HF solution and shaken overnight. The precipitate was collected by centrifugation and the HA was transferred to a dialysis tube until the dialysis water gave a negative Cl^- test with $AgNO_3$, and then the HA was freeze-dried. Next, 46% HF/2M HCl (1:1) was added to the HM, and the suspension

was shaken at 70–80 °C for 2–3 min. The precipitate was centrifuged for collection, and the HM residue was washed with deionized water and then freeze-dried to obtain the HM. The SAET for HA was conducted five times in this study. As the amount of HA decreased with the sequential extractions, HAs obtained during the first and second extraction were combined to give the sorbent HA1, and the HA fractions obtained during the third to fifth extractions were combined to give the sorbent HA2. This was required to fulfil the requirements for sorbent dosage in the experiments investigating SEs sorption to different HA fractions.

2.3. SEs detection and sorbent characterization

The solid phase extraction (SPE) and gas chromatography-mass spectrometry (GC-MS) approach previously developed by our team (Song et al., 2018) was applied for quantification of the E1 and 17β-E2 concentrations, and details on SEs detection were provided in the Supplementary Material (S1). The C, H, O, N, and S contents of the sorbent were analyzed using an Elementar Vario ELIII elemental analyzer (Germany). The solid-state cross-polarization magic angle-spinning ^{13}C NMR spectra of all sorbents were obtained with a Bruker Avance III 600 MHz NMR Spectrometer (Germany) operated at a ^{13}C frequency of 100 MHz. Surface elemental composition and carbon-based functionalities of the sorbent were determined using XPS (Thermo ESCALAB 250Xi, USA) with a monochromatic Al KR radiation source operated at 225 W, 15 mA, and 15kV. Spectrum processing was accomplished with the Xpspeak41 software to identify the functional group corresponding to the binding energy (Nguyen et al., 2009; Doskočil et al., 2015; Mylotte et al., 2015). FTIR (Perkin-Elmer 1725X) was used to analyze the functional groups in soil and its organic fractions, with a resolution of 4 cm^{-1} and measurement range of 4000–400 cme^{-1}. The surface area, micropore area, and micropore volume were used to examine the level of pore filling and calculated from the adsorption–desorption isotherm of N_2 at 77 K by the multipoint Brunauer–Emment–Teller (BET) method using a surface area and porosimetry analyzer (Micromeritics ASAP 2460, USA) (Xin et al., 2012).

187 *2.4. Batch sorption experiments*

188 The batch sorption experiments of E1 and 17β-E2 were conducted on soil
189 component fractions in screw-cap vials with aluminum foil and Teflon liners.
190 Background solutions consisted of 0.01 M $CaCl_2$ in deionized water to maintain a
191 constant ionic strength. The optimal liquid/solid phase ratio (25:1 for soil and 40:1 for
192 HA/HM) and initial SEs concentration range were determined through preliminary
193 experiments to obtain 20%–80% uptake of sorbate at equilibrium. For kinetic
194 experiments, the vials were placed in a thermostatic oscillator (150 rpm) for shaking
195 over 7 d at 25 ± 1 °C with sampling throughout. Preliminary tests indicated that
196 apparent sorption equilibrium was attained within 3 d. The equilibrium sorption tests
197 were hence equilibrated for 3 d with initial concentration of SEs within the range of
198 100–3000 μg/L. The supernatant was collected for SEs analysis after standing for 2 d.
199 Following the sorption experiments, the vials with initial concentrations of 500,
200 1000, and 2000 μg/L were used to determine the SEs desorption. Background solution
201 was added to each vial to begin the desorption study, and these desorption steps were
202 repeated three times. All samples, including blanks, were run in duplicate. Because of
203 the negligible mass loss of sorbates confirmed in the blanks (<2%), SEs sorption uptake
204 by all samples was calculated based on mass difference.

205 *2.5. Bioavailability experiment*

206 To explore the bioavailability of SEs under different sorption mechanisms and
207 aging conditions simultaneously, soil, HA1, and HM were pre-equilibrated with SEs
208 solutions (E1 or 17β-E2 1000 μg/L, 0.01 M $CaCl_2$) at 25 ± 1 °C for 3, 15, and 30 d in
209 dark, respectively. The soil, SOM and background solution were all autoclaved at
210 120 °C for 30 min three successive times in the aging processes to prevent SEs
211 biodegradation. Before the bioavailability experiment, the suspension was centrifuged
212 at 5000 rpm for 5 min, and then the supernatant was collected and an equal amount of
213 soil microbial suspension was added to the residues. The SEs content in supernatant
214 was detected to calculate the concentration of Ses sorbed on soil or SOM, which was
215 used as the initial concentration of bioavailability experiment. All treatments were

incubated in dark at 25 ± 1 °C, 150 rpm for 14 d. Samples containing both sorbent and aqueous phases were collected at different periods and analyzed using GC-MS to determine the biodegradation of SEs. Each treatment included two replicates.

2.6. Modelling of sorption kinetics and isotherms

The sorption kinetic data were fitted with a two-compartment first-order kinetic model (Johnson et al., 2001):

$$q_t = q_e\left[f_1\left(1-e^{-k_1 t}\right)+f_2\left(1-e^{-k_2 t}\right)\right], \quad (1)$$

where t [h] is the sorption reaction time; q_t [μg/g] is the SEs concentration in the sorbent at time t; q_e [μg/g] is the equilibrium concentration of SEs in the sorbent; k_1 and k_2 [1/h] are apparent first-order rate constants for the quick and slow sorption fractions, respectively; and f_1 and f_2 are the contribution rate of quick and slow sorption, respectively, where $f_1 + f_2 = 1$. The sorption equilibrium data were fitted with the logarithmic form of the Freundlich model:

$$\log q_e = \log K_f + n\log C_e, \quad (2)$$

where C_e [μg/L] is the equilibrium aqueous concentration; K_f [(μg/g)/(μg/L)^n] is the sorption coefficient; and n is a site energy heterogeneity factor, typically used as an isotherm nonlinearity indicator. The concentration dependence of the affinity of the SEs to the sorbent was analyzed by calculating the solid/liquid distribution coefficients (K_D, L/g) at concentrations (C_e) equal to the aqueous solubility (S_w) of solute (at $0.001S_w$, $0.01S_w$, and $0.1S_w$). The organic carbon content-normalized distribution coefficient (K_{oc}) was calculated as follows:

$$K_D = q_e/C_e, \quad (3)$$

$$K_{oc} = (K_D / \%\ \text{organic carbon}) \times 100. \quad (4)$$

The desorption hysteresis index (HI) was obtained by calculating the ratio of linear index of the sorption–desorption isotherm, which was fitted with the Freundlich model:

$$HI_i = N_{Di}/N_S, \quad (5)$$

where N_S and N_{Di} are the linear indexes of the sorption isotherm and desorption

243 isotherm, respectively.

244 The degradation of SEs was fitted to a first-order kinetic equation:

245 $$\ln C/C_0 = -kt, \quad (6)$$

246 where C_0 and C [μg/g] are concentration of SEs at the initial time and time t,
247 respectively, and k is the degradation rate constant. The half-life ($t_{1/2}$) of SEs was
248 computed from the rate constant using the following equation: $t_{1/2} = ln2/k$.

249 *2.7 Statistical analysis*

250 A one-way analysis of variation (ANOVA) and a least significant difference (LSD)
251 multiple comparisons ($p < 0.05$) were used to assess the significant difference among
252 different treatments (sorbents, SEs and so on). The Pearson correlation analysis was
253 performed to measure the pairwise relationship between different variables (i.e., TOC,
254 quick sorption, slow sorption, micropore volume and others).

255 **3. Results and discussion**

256 *3.1. Characteristics of SOM fractions*

257 The FTIR spectra of soil and its sequential alkaline-extraction fractions showed
258 some differences (Fig. 1). Observed functionality included (Pérez et al., 2004; Smidt et
259 al., 2007) the broad band at 3620 cm^{-1} ascribed to O-H stretching vibration; the peaks
260 at 2950 and 2860 cm^{-1} corresponding to aliphatic C-H stretching; the absorption peak
261 at 1710 cm^{-1} attributed to C=O stretching of COOH and ketones; and the peaks at 1450,
262 1510, and 1645 cm^{-1} attributed to structural vibrations of C=C within the aromatic ring
263 skeleton. In addition, the strong peak at 1030 cm^{-1} was associated with stretching
264 vibration of C-O in aromatic ethers, carbohydrates, or polysaccharides, and that at 1110
265 cm^{-1} was attributed to the stretching vibrations of C-O in aliphatic ethers. Thus, soil
266 and SOM fractions all contained prominent aliphatic carbon (3000–2800 cm^{-1})
267 alongside aromatic carbon (1640 cm^{-1}).

268 The aliphatic carbon and aromatic carbon accounted for 31.2%–43.9% of the total
269 organic carbon (TOC) in bulk SOM measured by the ^{13}C NMR (Table S2; Fig. 1), which

was low than their surface content of 54.8%–62.1% determined using XPS (Table S2; Fig. S1). These results indicated that more other O-containing polar functionalities were distributed within the SOM interior, which was demonstrated by the higher bulk polarity (O+N/C) compared with the surface polarity (Table S2). The total aliphatic carbon content of bulk (0–109 ppm) and surface both increased with the sequential extraction of HA (Table S2; Fig. 1), but aromatic carbon and O-containing polar functionalities contents declined. Together these results indicate that aliphatic carbon is more strongly bound to soil minerals than aromatic carbon (Zhang et al., 2014; Yang et al., 2012; Wang et al. 2011). The increasing C/N values (taken to be indicative of higher stability of SOM) indicated that stability increased with HA isolation (HA1 < HA2 < HM; Table 1) (Zhu et al., 2005). Our work is consistent with previous studies that showed that stability, compacted structure, condensation degree, and intermolecular intersections of SOM increase in the following order: HA < HM < kerogen < black carbon (Yang et al., 2004; Cornelissen et al., 2005).

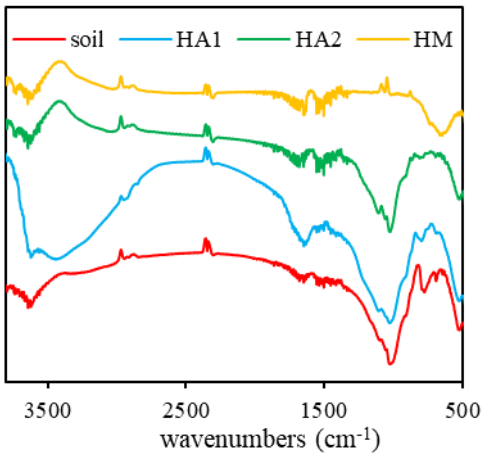

Fig. 1. FTIR spectra of soil, HAs (HA1 and HA2), and HM.

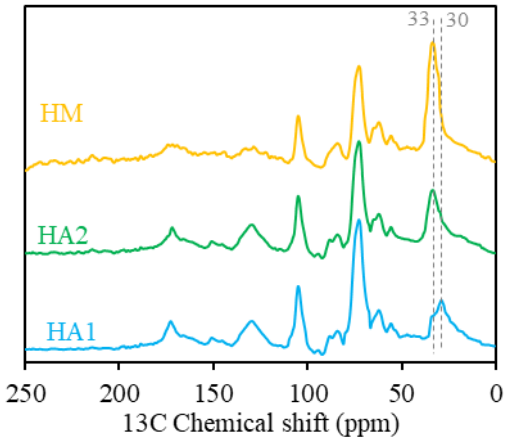

Fig. 2. Solid-state ^{13}C NMR spectra of HAs (HA1, HA2) and HM.

3.2. Slow sorption, sorption nonlinearity, and desorption hysteresis

Rates of E1 and 17β-E2 sorption on soil components were relatively high, with 80% of the equilibrium sorption capacity reached within 24 h and the apparent sorption equilibrium attained in 72 h (Table 1, Fig. 3). A typical two-stage process of quick sorption was evident, followed by a slow sorption process (Fig. 3). Quick sorption accounted for over 70% of sorbed mass occurring within 12 h (except for HM).

290 Thereafter, the contribution rate of slow sorption gradually increased until the sorption
291 equilibrium was achieved. The quick sorption rate constant k_1 exceeded the slow
292 sorption rate constant k_2 by 1–2 orders of magnitude (Table 1). For the same sorbent,
293 the contribution rate of slow sorption (f_2) of 17β-E2 was slightly higher than that of E1.
294 Comparison of the f_2 value of SEs in different sorbents showed that the f_2 of HM and
295 soil were highest, but quick sorption dominated in HA1 (Table 1). This also supports
296 the influence of progressive SOM fractionation on SEs sorption; with the sequential
297 extraction of SOM from HA1, HA2, and then HM, SEs sorption shifted from quick
298 sorption (f_1) dominance to increasing slow sorption (f_2) contributions reaching similar
299 levels.

300 **Table 1**

301 Two-compartment first-order kinetics model parameters for E1 and 17β-E2 sorption in
302 soil and SOM.

Sorbent	E1					17β-E2				
	k_1	k_2	f_1	f_2	R^2	k_1	k_2	f_1	f_2	R^2
Soil	3.93	0.09	0.51	0.49	0.999	2.81	0.05	0.49	0.51	0.998
HA1	4.92	0.10	0.74	0.26	0.996	9.30	0.11	0.69	0.31	0.998
HA2	0.88	0.05	0.69	0.31	0.986	0.60	0.03	0.46	0.54	0.995
HM	13.61	0.09	0.49	0.51	0.980	15.35	0.16	0.48	0.52	0.982

303

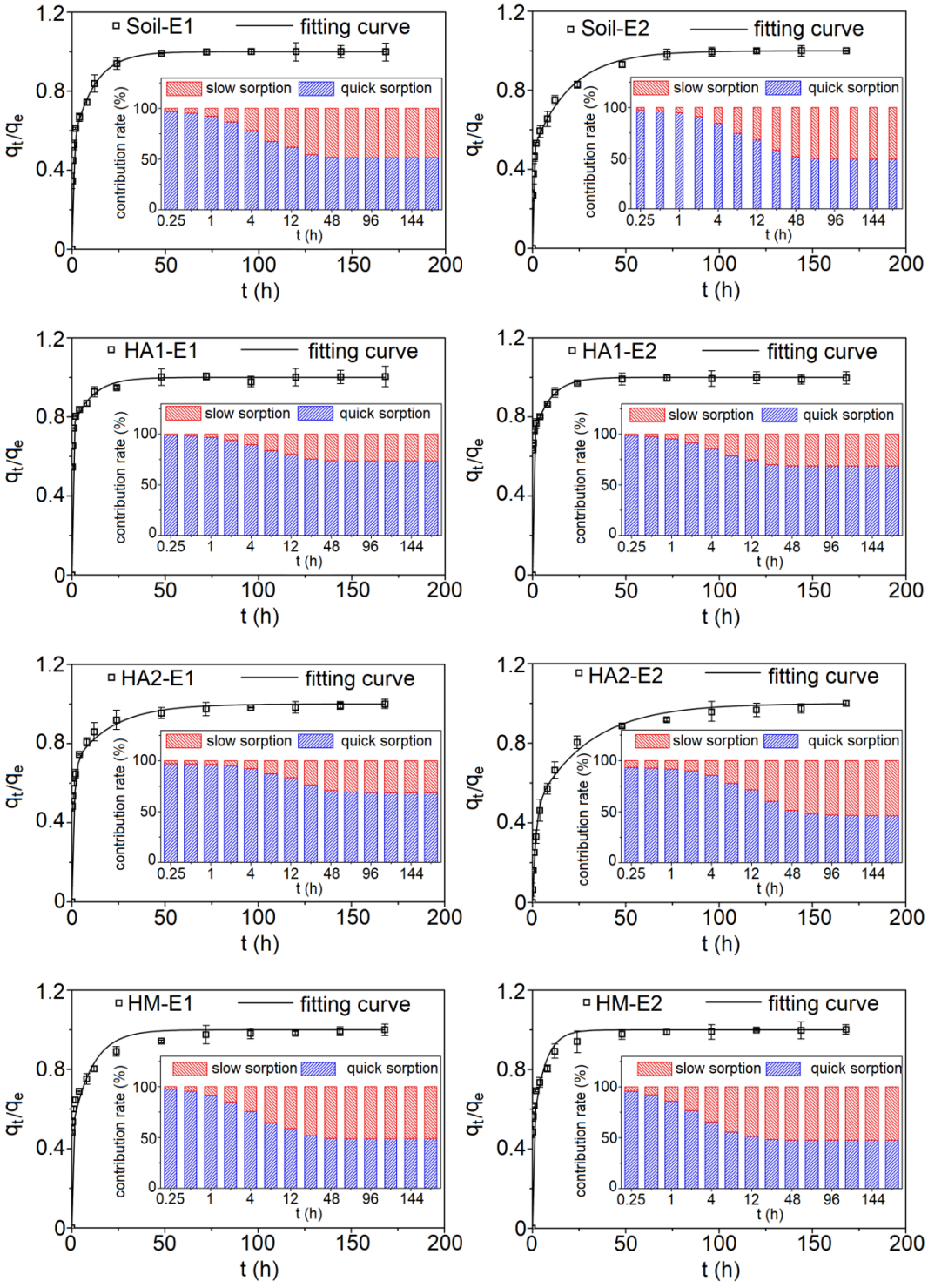

Fig. 3. The batch data and simulated two-compartment first-order kinetic model fittings of E1 and 17β-E2 sorbed on soil and SOM, with inset graphs showing the simulated quick and slow sorption rate contributions.

The sorption and desorption processes fitted well to the Freundlich equation (all $R^2 > 0.96$) (Fig. 4 and S2; Tables S3 and S4), which is consistent with previous SEs

sorption studies. Nonlinear sorption isotherms with $n < 1$ were obtained for both SEs, especially in soil and HM. The n value of E1 was greater than that of 17β-E2 (except for HA2) with the same sorbent (Table S3), and hence nonlinear sorption of 17β-E2 was more evident. The sorption nonlinearity of humic substances also increased with the sequential extraction of HA, consistent with the increased contribution rate of slow sorption (f_2). It is reasonable to suggest that slow sorption was primarily responsible for the observed nonlinear sorption. The sorption capacity also increased with sequential HA extraction (Table S3). The logK_{oc} values of 17β-E2 were higher than those for E1, consistent with its greater hydrophobicity. The desorption hysteresis index (*HI*) was positively correlated with initial SEs concentration (Table S4). A consistently slightly lower *HI* of 17β-E2, when compared to E1 for the same sorbent, indicates its greater desorption hysteresis, and hence its more difficult desorption with a higher proportion of irreversible sorption sites. The *HI* values of sorbents increased with sequential HA extraction, indicating that desorption became increasingly difficult and the proportion of irreversible sorption sites also increased.

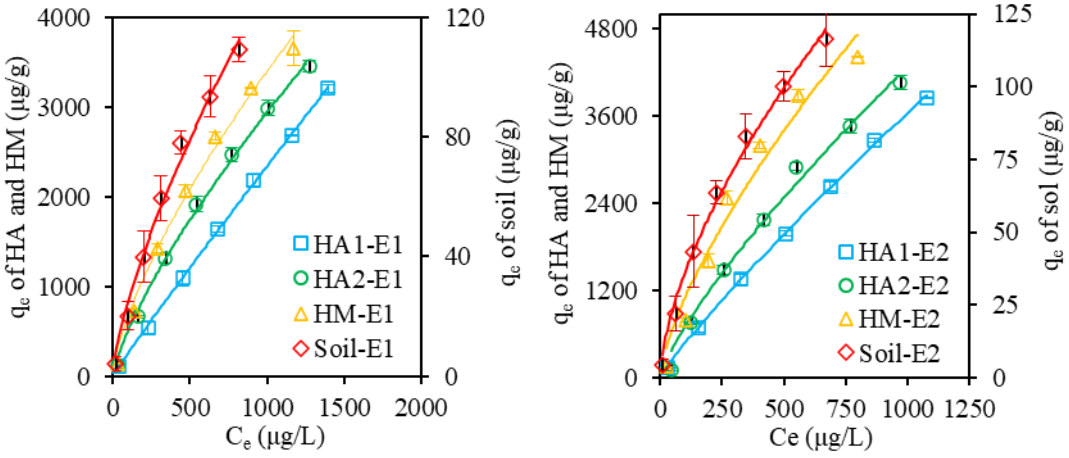

Fig. 4. Freundlich sorption isotherms of E1 and 17 β -E2 by soil, HAs and HM, respectively.

3.3. Impact of sorbent elemental composition, polarity, functionality, and spatial arrangement

The logK_{oc} of E1 and 17β-E2 by soil and humic substances was positively correlated with TOC ($p < 0.05$) (Fig. 5a and 5b), and the logK_{oc} of 17β-E2 was higher than that of E1, which was consistent with a higher logK_{ow} value of 17β-E2 compared

with E1 (Fig. 5c). The hydrophobic interaction of SEs in SOM hence played a critical role in their sorption. With the sequential extraction of SOM, the logK_{oc}/logK_{ow} value of 17β-E2 was slightly higher than that of E1 in soil and HA1, but with the opposing trend found in HA2 and HM (Fig. 5d). This was probably related to the functionality composition of hydrophobic organic compounds generally (including SEs) and their interaction with the specific sorption sites (such as hydrogen bonds and π-π bonds) of condensed organic matter in soil (Zhu et al., 2004, 2005; Sun et al., 2010; Takigami et al., 2011).

Linear and quick sorption of HOCs is generally expected in the SOM amorphous organic matter domain, and nonlinear, slow sorption to the crystalline SOM (Huang et al., 1997; Johnson et al., 2001). The ^{13}C NMR spectra of humic substances showed that the crystalline carbon (33 ppm) became more prominent compared with amorphous carbon (30 ppm) with the increased sequential extraction of humic substances (Fig. 2) (Chen et al., 2017). The nonlinear sorption can hence be ascribed to the increase in condensed organic matter content and the influence of these sorption sites. However, the nonlinearity (n) of SEs in the bulk soil was also relatively high, which can be reasonably ascribed to the complicated composition and structure and increased heterogeneity. The chemical π-π interactions and hydrogen bonding also contributed to the nonlinear sorption due to the aromatic ring, hydroxyl, and ketone groups for both E1 and 17β-E2 molecules (Kim et al., 2016). However, hydroxyl groups may form stronger hydrogen bonds than their ketone counterparts, and the two hydroxyls within 17β-E2, versus E1's single hydroxyl and single ketone group, may cause increased hydrogen bonding of the former to the SOM and explain the greater nonlinearity of 17β-E2 sorption observed. Therefore, the contents of SOM and its hydrophobic distribution are the decisive factors controlling SEs adsorption capacity; however, the difference in molecular structure between E1 and 17β-E2 and their specific sorption on SOM via the hydrogen bond and π-π bond resulted in the different sorption nonlinearity.

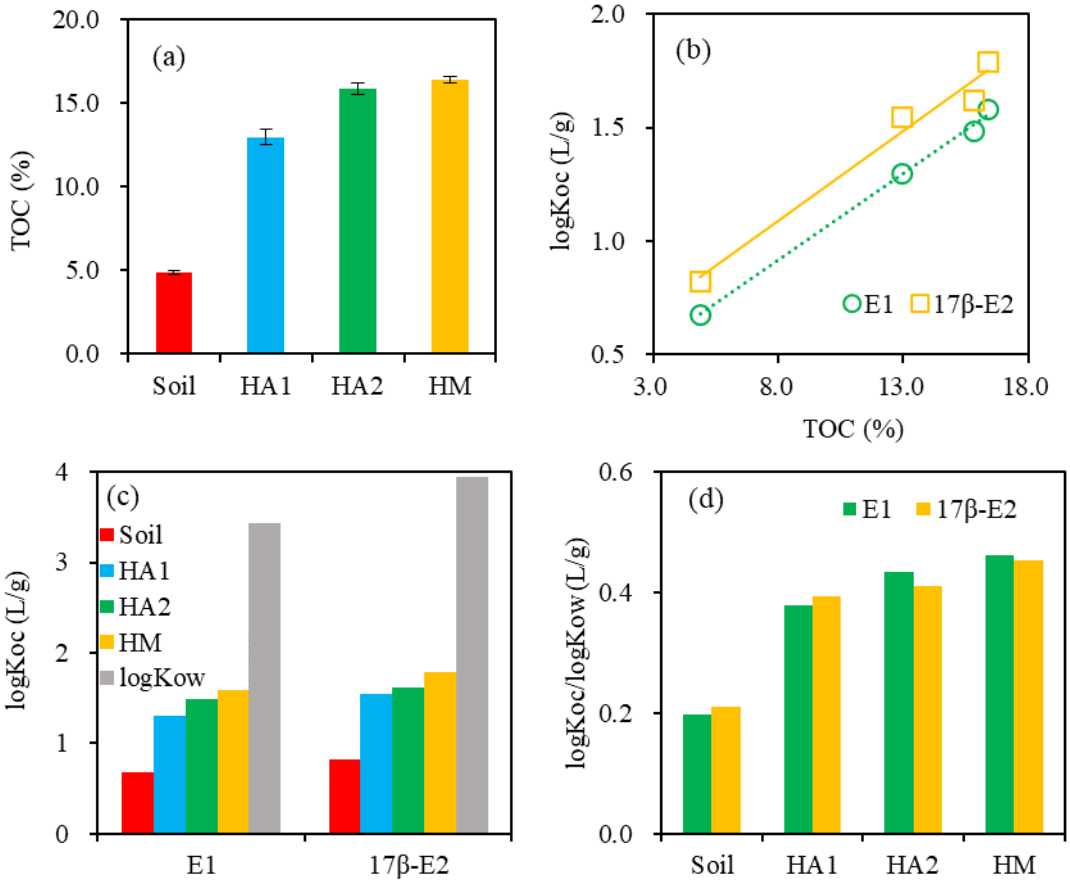

Fig. 5. Characteristics of humic substances and their sorption: (a) TOC variation; (b) correlations between TOC and sorption capacity of SEs (logK_{oc}); (c) relationship between their octanol-water partition coefficient (logK_{ow}) and logK_{oc} values of SEs; and (d) logK_{oc}/ logK_{ow} values of E1 and 17β-E2 in soil and humic substances.

Micropore area and volume of sorbents can be used to examine the sorption mechanism of pore filling, which is the main process responsible for slow sorption and subsequent desorption hysteresis due to accessibility constraints (Pan et al., 2006). The contribution rate of the slow sorption of SEs in soil and SOM were positively related to the micropore volumes of sorbents ($R^2 > 0.80$, $p < 0.05$), but poorly correlated with TOC content ($R^2 < 0.1$, $p > 0.05$) (Fig. S3a–d). It can be concluded that the slow sorption was mainly induced by pore filling. The micropore volumes of sorbents was negatively correlated with *HI* ($p < 0.05$) (Fig. S3d). It is speculated that more SEs can enter the sorption sites in micropores with larger micropore volumes, which cannot desorb, leading to enhanced desorption hysteresis (Dai et al., 2022). The sorption capacity

($\log K_{oc}$) of SEs was negatively correlated with the surface and bulk polarity of sorbents ($p < 0.05$) (Fig. S3e, f). Sorbents of higher polarity generally contain abundant hydrophilic oxygen-containing moieties, which can provide sites for water cluster formation at their surface through H-bonding (Wang et al., 2011). Water clusters may further reduce the surface hydrophobicity of sorbents and the accessibility of those HOCs to sorption sites, as well as compete with them; thus, the sorption of both E1 and 17β-E2 may be blocked by the high polar components on the sorbent surface. The $\log K_{oc}$ of E1 and 17β-E2 was positively correlated with bulk alkyl carbon in SOM ($p < 0.05$) (Fig. S3g), which demonstrated that the aliphatic carbon content of SOM was a key factor regulating the sorption of SEs. Although the soil had the highest bulk H/C, its TOC content was the lowest of the studied sorbents, resulting in the lowest $\log K_{oc}$ value. This further indicated that SOM was the main factor controlling SEs sorption in soil. The ratio of surface aliphatic carbon was lower than the bulk, indicating that the aliphatic carbon was mainly distributed in the interior parts of sorbent rather than at the surface. The sorption capacity ($\log K_{oc}$) of E1 and 17β-E2 was also positively correlated with the content of aliphatic carbon of the sorbent surface and negatively correlated with the content of surface aromatic carbon (Fig. S3h), which further demonstrates that the content of aliphatic carbon in SOM and the conformation of SOM were the key factors governing SEs sorption. The overall impact of sorbent elemental composition, polarity, functionalities, and their spatial arrangement on SEs sorption was significant and complex. Especially, the spatial arrangement characteristics of functionalities by the increase of surface hydrophobic alkyl carbon, and the decrease of surface polarity with sequential alkaline-extraction of SOM contributed to more SEs sorption.

3.4. Response of SEs bioavailability to sorption and aging processes with SOM

The biodegradation of E1 and 17β-E2 in soil, HA1, and HM were well fitted with the first-order degradation kinetics model ($R^2 > 0.85$) (Fig. 6; Table S5). The degradation rate constant (k) and degradation ratio of SEs showed no significant correlation with the TOC of the sorbent ($p > 0.05$) (Fig. S4), indicating that the difference in SE biodegradation in soil and SOM could not be attributed to the TOC

content. The HOCs are first sorbed on the soil surface, into the large pores, or through hydrophobic interaction into amorphous organic matter of SOM. This is followed by the slow and gradual adsorption of SEs into micropores or condensed organic matter of SOM that cannot be entered by microorganisms. Therefore, it could be inferred that the bioavailability of SEs by quick sorption is higher than that of slow sorption. The content of condensed organic matter increases with sequential alkaline-extraction, and the *k* value and degradation ratio of E1 and 17β-E2 were both positively correlated with the contribution rate of fast sorption, but negatively correlated with the contribution rate of slow adsorption (Table 2). This indicates that the rapid degradation in the early stage is associated with the SEs in the dissolved phase or in fast sorption, as both gradually reduce as the degradation rate decreases. Subsequently, the SEs of slow sorption are used by microorganisms until desorption stops, giving a stable degradation ratio. This further indicates that the irreversible sorption and strong desorption hysteresis of estrogen on HM with the maximum content of condensed matter organic carbon and micropore volume contribute to the low bioavailability, which is the key controlling factor led to the differences in SEs bioavailability among these sorbents. Overall, these results suggested that the hydrophobic interaction was the key mechanism of SEs sorption and was characterized with quick sorption and high bioavailability. However, micropore filling and its specific sorption in condensed SOM were likely the main cause of the slow or irreversible sorption and desorption hysteresis, which also contributed to the low bioavailability.

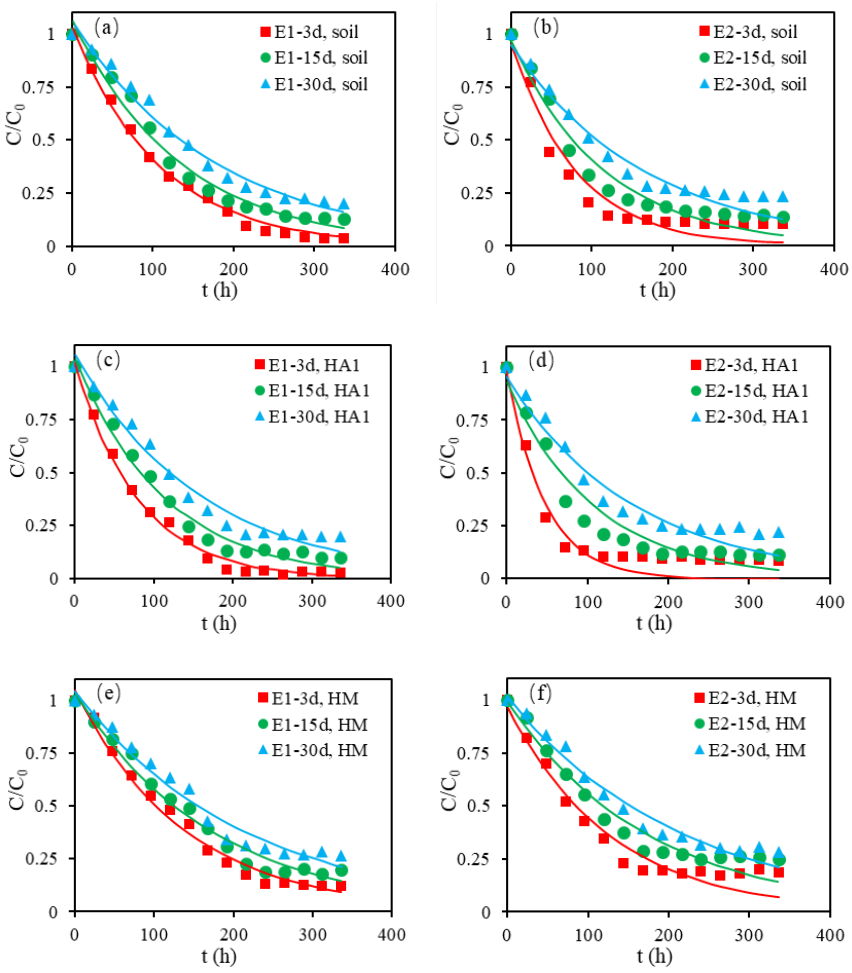

Fig. 6. Effect of the aging time (3 d, 15 d, and 30 d) on E1 and 17β-E2 degradation in soil and SOM fractions (HA1 and HM).

With the increase of aging time, the bioavailability and biodegradation rate constant decreased, and the degradation half-life increased (Table S5). In the aging process, the bioavailability of SEs was greatly reduced because the SEs have more time to diffuse into soil micropores and condensed organic matter, leading to an increase in the proportion of irreversible sorption and the blocking of the exposure pathway of SEs to microorganisms. This is confirmed by the well-developed micropores and high content of condensed organic matter in HM. For the same sorbent, the degradation rate of 17β-E2 was lower than that of E1 at different aging times. This may be related to the strong hydrophobicity of 17β-E2 and its strong affinity with soil and SOM. In addition, the 17β-E2 molecule contains two hydroxyl groups and has a stronger specific binding

ability (such as hydrogen bonding) to sorbents than E1, which may be the reason for the lower bioavailability of 17β-E2.

Table 2

Relationship between sorption kinetic parameters and degradation kinetic parameters after aging 3 days.

SEs	sorbents	k (h^{-1})	degradation ratio (%)	contribution rate of quick sorption	contribution rate of slow sorption
E1	HM	0.007	88.0	0.49	0.51
	Soil	0.009	96.3	0.51	0.49
	HA1	0.012	97.2	0.74	0.26
17β-E2	HM	0.008	81.5	0.48	0.52
	Soil	0.012	89.8	0.49	0.51
	HA1	0.021	91.7	0.69	0.31

4. Conclusions

Application of soil sequential extraction techniques provide an important means of assessing the contributions of the various SOM components to the sorption, desorption, and bioavailability of SEs in real agricultural soils. These findings provide an improved understanding of the risks posed to agricultural environment by SEs. The sorption of E1 and 17β-E2 was dominated by hydrophobic partitioning and quick sorption. However, this does not negate the importance of other sorption mechanisms. Specific sorption (hydrogen bond and π-π bond) interactions of SEs with the SOM and micropore filling were responsible for nonlinear and slow sorption, as well as desorption hysteresis. There was a significant effect of sorption on the bioavailability of SEs. In particular, the irreversible sorption in microporous and condensed organic matter improved the environmental persistence of SEs. This effect was significantly enhanced with an increase in aging time.

The gradual accumulation and distribution of SEs in agricultural soils receiving manures, and the potentially greatly delayed release of SEs, are each influenced by the balance between sorption on the SOM composition and the degradation of microorganisms. Even with assumptions of simple linear sorption control, lag times of

decades have been predicted by Gall et al. (2016) for the release of SEs from agricultural soils, with attendant risks posed over these timeframes to groundwater. The results of the current study suggest that these timeframes will be further extended because of the need to additionally consider the hysteretic, slow, non-linear desorption of SEs from the soil matrix. In particular, a fraction of SEs is subjected to pore filling sorption within any crystalline carbon present, which was characterized by high persistence due to the low bioavailability. Under these conditions, establishing the SEs sorption on different SOM fractions associated with the response of SEs bioavailability is necessary to predict the long-term risks of SEs in agricultural environment.

CRediT authorship contribution statement

Xiaoming Song: Experiment, Data curation, Writing - original draft, Writing - review & editing. **Zhipeng Zhang:** Experiment, Data curation, Writing - review & editing. **Yujuan Wen:** Experiment & SEs detection. **Wei Zhang:** Writing - review & editing. **Yi Xie:** Modeling. **Nan Cao**: Data curation, Formal analysis. **Dong Sun**: Data curation. **Yuesuo Yang:** Writing - review & editing, Supervision.

Declaration of competing interest

We declare that the research was conducted in the absence of any commercial or financial relationships that could be constructed as a potential conflict of interest.

Acknowledgements

This work was financially supported by National Key R&D Program of China (No. 2019YFC1804805), Key R&D Program of Liaoning Province (No. 2020JH2-10300083), the National Natural Science Foundation of China (No. 42172284), Liao Ning Revitalization Talents Program (XLYC1807259).

Appendix A. Supplementary data

References

Adeel, M., Song, X., Wang, Y., Francis, D., Yang, Y., 2017. Environmental impact of estrogens on human, animal and plant life: a critical review. Environ. Int. 99, 107-119.

Alizadeh, S., Prasher, S.O., ElSayed, E., Qi, Z., Patel, R.M., 2018. Effect of biochar on fate and transport of manure-borne estrogens in sandy soil. J. Environ. Sci. 73, 162-176.

Bedard, M., Giffear, K.A., Ponton, L., Sienerth, K.D., Moore, V.D.G., 2014. Characterization of binding between 17β-estradiol and estriol with humic acid via NMR and biochemical Analysis. Biophys. Chem. 189, 1-7.

Chen, W., Wang, H., Gao, Q., Chen, Y., Li, S., Yang, Y., Werner, D., Tao, S., Wang, X., 2017. Association of 16 priority polycyclic aromatic hydrocarbons with humic acid and humin fractions in a peat soil and implications for their long-term retention. Environ. Pollut. 230, 882-890.

Citulski, J.A., Farahbakhsh, K., 2010. Fate of endocrine-active compounds during municipal biosolids treatment: a review. Environ. Sci. Technol. 44 (22), 8367-8376.

Combalbert, S., Hernandez-Raquet, G., 2010. Occurrence, fate, and biodegradation of estrogens in sewage and manure . Appl. Microbiol. Biot. 86,1671-1692.

Cornelissen, G., Gustafsson, Ö., Bucheli, T.D., Jonker, M.T., Koelmans, A.A., van Noort, P.C., 2005. Extensive sorption of organic compounds to black carbon, coal, and kerogen in sediments and soils: mechanisms and consequences for distribution, bioaccumulation, and biodegradation. Environ. Sci. Technol. 39 (18), 6881-6895.

Dai, X., Yang, X., Xie, B., Jiao, J., Jiang, X., Chen, C., Zhang, Z., He, Z., Lin, H., Chen, W., Li, Y., 2022. Sorption and desorption of sex hormones in soil-and sediment-water systems: A review. Soil. Ecol. Lett. 4, 1-17.

Doskočil, L., Grasset, L., Enev, V., Kalina, L., Pekař, M., 2015. Study of water-extractable fractions from South Moravian lignite. Environ. Earth. Sci. 73 (7), 3873-3885.

Fang, T.Y., Praveena, S.M., Aris, A.Z., Ismail, S.N.S., Rasdi, I., 2016. Analytical techniques for steroid estrogens in water samples-A review. Chemosphere. 165, 358-368.

Fan, Z., Casey, F.X.M., Hakk, H., Larsen, G.L., 2007. Discerning and modeling the fate and transport of testosterone in undisturbed soil. J. Environ. Qual. 36 (3), 864-873.

Gall, H.E., Sassman, S.A.; Jenkinson, B., Lee, L.S., Jafvert, C.T., 2015. Comparison of

export dynamics of nutrients and animal-borne estrogens from a tile-drained Midwestern agroecosystem. Water. Res. 72, 162-173.

Gall, H.E., Basu, N.B., Mashtare, M.L., Rao, P.S.C., Lee, L.S., 2016. Assessing the impacts of anthropogenic and hydro-climatic drivers on estrogen legacies and trajectories. Adv. Water. Resour. 87, 19-28.

Gámiz. B., Velarde, P., Spokas, K.A., Celis, R., Cox, L., 2018. Changes in sorption and bioavailability of herbicides in soil amended with fresh and aged biochar. Geoderma. 337, 341-349.

Huang, W., Weber, W.J., 1997. A distributed reactivity model for sorption by soils and sediments. 10. Relationships between desorption, hysteresis, and the chemical characteristics of organic domains. Environ. Sci. Technol. 31 (9), 2562-2569.

Jiang, L., Liu, Y., Liu, S., Zeng, G., Hu, X., Hu, X., Wu, Z., 2017. Adsorption of estrogen contaminants by graphene nanomaterials under natural organic matter preloading: comparison to carbon nanotube, biochar, and activated carbon. Environ. Sci. Techno. 51 (11), 6352-6359.

Johnson, M.D., Keinath, T.M., Weber, W.J., 2001. A distributed reactivity model for sorption by soils and sediments. 14. Characterization and modeling of phenanthrene desorption rates. Environ. Sci. Technol. 35 (8), 1688-1695.

Karnjanapiboonwong, A., Morse, A.N., Maul, J.D., Anderson, T.A., 2010. Sorption of estrogens, triclosan, and caffeine in a sandy loam and a silt loam soil. J. Soil. Sediment. 10 (7), 1300-1307.

Kim, E., Jung, C., Han, J., Her, N., Park, C., Jang, M., Yoon, Y., 2016. Sorptive removal of selected emerging contaminants using biochar in aqueous solution. J. Ind. Eng. Chem. 36, 364-371.

Lee, J.H., Zhou, J.L., Kim, S.D, 2011. Effects of biodegradation and sorption by humic acid on the estrogenicity of 17β-estradiol. Chemosphere, 85 (8), 1383-1389.

Lima, D.L., Schneider, R.J., Esteves, V.I., 2012. Sorption behavior of EE2 on soils subjected to different long-term organic amendments. Sci. Total. Environ. 423, 120-124.

Mashtare, M.L., Khan, B., Lee, L.S., 2011. Evaluating stereoselective sorption by soils of 17α-estradiol and 17β-estradiol. Chemosphere. 82 (6), 847-852.

Mylotte, R., Verheyen, V., Reynolds, A., Dalton, C., Patti, A.F., Chang, R.R., Hayes, M.H., 2015. Isolation and characterisation of recalcitrant organic components from an estuarine sediment core. J. Soil. Sediment. 15 (1), 211-224.

559 Nguyen, B.T., Lehmann, J., Kinyangi, J., Smernik, R., Riha, S.J., Engelhard, M.H.,
560 2009. Long-term black carbon dynamics in cultivated soil. Biogeochemistry. 92
561 (1-2), 163-176.
562 Pan, B., Xing, B., Liu, W., Tao, S., Lin, X., Zhang, Y., Xiao, Y., 2006. Two-
563 compartment sorption of phenanthrene on eight soils with various organic carbon
564 contents. J. Environ. Sci. Heal. B. 41 (8), 1333-1347.
565 Pérez, M.G., Martin-Neto, L., Saab, S.C., Novotny, E.H., Milori, D.M., Bagnato, V.S.,
566 Knicker, H., 2004. Characterization of humic acids from a Brazilian Oxisol under
567 different tillage systems by EPR, 13 C NMR, FTIR and fluorescence spectroscopy.
568 Geoderma. 118 (3), 181-190.
569 Sangster, J.L., Oke, H., Zhang, Y., Bartelt-Hunt, S.L., 2015. The effect of particle size
570 on sorption of estrogens, androgens and progestagens in aquatic sediment. J.
571 Hazard. Mater. 299, 112-121.
572 Shi, W., Li, S., Chen, B., Wang, C., Sun, W., 2017. Effects of Fe_2O_3 and ZnO
573 nanoparticles on 17β-estradiol adsorption to carbon nanotubes. Chem. Eng. J. 326,
574 1134-1144.
575 Smidt, E., Meissl, K., 2007. The applicability of Fourier transform infrared (FT-IR)
576 spectroscopy in waste management. Waste. Manage. 27 (2), 268-276.
577 Song, X., Wen, Y., Wang, Y., Adeel, M., Yang, Y., 2018. Environmental risk
578 assessment of the emerging EDCs contaminants from rural soil and aqueous
579 sources: Analytical and modelling approaches. Chemosphere. 198, 546-555.
580 Stumpe, B., Marschner, B., 2010. Organic waste effects on the behavior of 17β-
581 estradiol, estrone, and 17α-ethinylestradiol in agricultural soils in long-and short-
582 term setups. J. Environ. Qual. 39 (3), 907-916.
583 Sun, K., Ran, Y., Yang, Y., Xing, B., 2008. Sorption of phenanthrene by
584 nonhydrolyzable organic matter from different size sediments. Environ. Sci.
585 Technol. 42 (6), 1961-1966.
586 Sun, K., Gao, B., Zhang, Z., Zhang, G., Liu, X., Zhao, Y., Xing, B., 2010. Sorption of
587 endocrine disrupting chemicals by condensed organic matter in soils and sediments.
588 Chemosphere. 80 (7), 709-715.
589 Sun, K., Jin, J., Gao, B., Zhang, Z., Wang, Z., Pan, Z., Xu, D., Zhao, Y., 2012. Sorption
590 of 17α-ethinyl estradiol, bisphenol A and phenanthrene to different size fractions
591 of soil and sediment. Chemosphere. 88 (5), 577-583.
592 Sun, W., Wang, C., Pan, W., Li, S., Chen, B., 2017. Effects of natural minerals on the

593 adsorption of 17β-estradiol and bisphenol A on graphene oxide and reduced
594 graphene oxide. Environ. Sci-Nano. 4 (6), 1377-1388.
595 Swift, R.S., 1996. Organic matter characterization (chap 35). In D.L. Soarks et al. (Eds.)
596 Method of soil analysis. Part 3. Chemical methods. Soil Science Society of
597 America. Madison, Wisconsin, USA. 1018-1020.
598 Takigami, H., Taniguchi, N., Shimizu, Y., 2011. Sorption and desorption of 17β-
599 estradiol to natural sediment. Water. Sci. Technol. 64 (7), 1473-1478.
600 Thanhmingliana, T., Lalhriatpuia, C., Tiwari, D., Lee, S.M., 2016. Efficient removal of
601 17β-estradiol using hybrid clay materials: Batch and column studies. Environ. Eng.
602 Res. 21 (2), 203-210.
603 Tong, X., Li, Y., Zhang, F., Chen, X., Zhao, Y., Hu, B., Zhang, X., 2019. Adsorption
604 of 17β-estradiol onto humic-mineral complexes and effects of temperature, pH, and
605 bisphenol A on the adsorption process. Environ. Pollut. 254, 112924.
606 Wang, J., Bao, H., Pan, G., Zhang, H., Wu, F., 2021. Combined application of
607 rhamnolipid and agricultural wastes enhances pahs degradation via increasing their
608 bioavailability and changing microbial community in contaminated soil. J. Environ.
609 Manage. 294 (9), 112998.
610 Wang, X., Guo, X., Yang, Y., Tao, S., Xing, B., 2011. Sorption mechanisms of
611 phenanthrene, lindane, and atrazine with various humic acid fractions from a single
612 soil sample. Environ. Sci. Technol. 45 (6), 2124-2130.
613 Wei, Z., Wang, J., Fultz, L., White, P., Jeong, C., 2020. Application of biochar in
614 estrogen hormone-contaminated and manure-affected soils: Impact on soil
615 respiration, microbial community and enzyme activity. Chemosphere.
616 Xin, J., Liu, X., Jiang, L., Li, M., 2012. BDE-47 sorption and desorption to soil matrix
617 in single-and binary-solute systems. Chemosphere. 87 (5), 477-482.
618 Xu, Y., Yu, X., Xu, B., Peng, D., Guo, X., 2020. Sorption of pharmaceuticals and
619 personal care products on soil and soil components: Influencing factors and
620 mechanisms. Sci. Total. Environ. 753.
621 Xu, Z., Xu, X., Tsang, D., Cao, X., 2018. Contrasting impacts of pre- and post-
622 application aging of biochar on the immobilization of cd in contaminated soils.
623 Environ. Pollut. 242, 1362-1370.
624 Yang, C., Huang, W., Xiao, B., Yu, Z., Peng, P.A., Fu, J., Sheng, G., 2004.
625 Intercorrelations among degree of geochemical alterations, physicochemical

626 properties, and organic sorption equilibria of kerogen. Environ. Sci. Technol. 38
627 (16), 4396-4408.
628 Yang, X., He, X., Lin, H., Lin, X., Mo, J., Chen, C., Li, Y., 2021. Occurrence and
629 distribution of natural and synthetic progestins, androgens, and estrogens in soils
630 from agricultural production areas in China. Sci. Total. Environ. 751.
631 Yang, Y., Saiers, J.E., Xu, N., Minasian, S.G., Tyliszczak, T., Kozimor, S.A., Barnett,
632 M.O., 2012. Impact of natural organic matter on uranium transport through
633 saturated geologic materials: from molecular to column scale. Environ. Sci.
634 Technol. 46 (11), 5931-5938.
635 Yu, W., Du, B., Fan, G., Yang, S., Yang, L., Zhang, M., 2020. Spatio-temporal
636 distribution and transformation of 17α-and 17β-estradiol in sterilized soil: A
637 column experiment. J. Hazard. Mater. 389.
638 Zhang, F., Li, Y., Zhang, G., Li, W., Yang, L., 2017. The importance of nano-porosity
639 in the stalk-derived biochar to the sorption of 17β-estradiol and retention of it in
640 the greenhouse soil. Environ. Sci. Pollut. R. 24 (10), 9575-9584.
641 Zhang, F., Yang, L., Liu, X., Li, Y., Fang, H., Wang, X., Li, J., 2018. Sorption of 17β-
642 estradiol to the dissolved organic matter from animal wastes: effects of composting
643 and the role of fulvic acid-like aggregates. Environ. Sci. Pollut. R. 25 (17): 16875-
644 16884.
645 Zhang, P., Ren, C., Sun, H., Min, L., 2018. Sorption, desorption and degradation of
646 neonicotinoids in four agricultural soils and their effects on soil microorganisms.
647 Sci. Total. Environ. 615, 59-69.
648 Zhao, L., Rong, L., Xu, J., Lian, J., Wang, L., Sun, H., 2020. Sorption of five organic
649 compounds by polar and nonpolar microplastics. Chemosphere. 257.
650 Zhao, X., Grimes, K.L., Colosi, L.M., Lung, W.S., 2019. Attenuation, transport, and
651 management of estrogens: a review. Chemosphere. 230, 462-478.
652 Zheng, W., L,i X., Yates, S.R., Bradford. S.A., 2012. Anaerobic transformation kinetics
653 and mechanism of steroid estrogenic hormones in dairy lagoon water. Environ. Sci.
654 Technol. 46 (10), 5471-5478.
655 Zhu, D., Hyun, S., Pignatello, J.J., Lee, L.S., 2004. Evidence for π - π electron donor–
656 acceptor interactions between π-donor aromatic compounds and π-acceptor sites in
657 soil organic matter through pH effects on sorption. Environ. Sci. Technol. 38 (16),
658 4361-4368.
659 Zhu, D., Pignatello, J.J., 2005. Characterization of aromatic compound sorptive

660 interactions with black carbon (charcoal) assisted by graphite as a model. Environ.
661 Sci. Technol. 39 (7), 2033-2041.
662 Zhu, Y., Li, A.M., Li, C., Dai, J.Y., 2005. Chracteristics of Soil Humic Substances by
663 Infrared Spectra and Thermal Gravity. Environ. Chem. 24 (3), 288-292.